Charge-noise tolerant exchange gates of singlet-triplet qubits in asymmetric double quantum dots

Tuukka Hiltunen,[1] Hendrik Bluhm,[2] Sebastian Mehl,[2,3] and Ari Harju[1]

[1]*COMP Centre of Excellence, Department of Applied Physics, Aalto University, Helsinki, Finland*
[2]*JARA-Institute for Quantum Information, RWTH Aachen University, D-52056 Aachen, Germany*
[3]*Peter Grünberg Institute (PGI-2), Forschungszentrum Jülich, D-52425 Jülich, Germany*

In the semiconductor double quantum dot singlet-triplet qubit architecture, the decoherence caused by the qubit's charge environment poses a serious obstacle towards large scale quantum computing. The effects of the charge decoherence can be mitigated by operating the qubit in the so-called sweet spot regions where it is insensitive to electrical noise. In this paper, we propose singlet-triplet qubits based on two quantum dots of different sizes. Such asymmetric double quantum dot systems allow the implementation of exchange gates with controllable exchange splitting J operated in the doubly occupied charge region of the larger dot, where the qubit has high resilience to charge noise. In the larger dot, J can be quenched to a value smaller than the intradot tunneling using magnetic fields, while the smaller dot and its larger splitting can be used in the projective readout of the qubit.

I. INTRODUCTION

The two-electron unpolarized singlet and triplet states in semiconductor double quantum dots (DQDs) are a promising scalable realization for a quantum bit [1,2]. The universal set of qubit operations [3–6] in this architecture includes one-qubit rotations generated by electrically detuning the two dots of the DQD system. These exchange rotations are dephased due to the charge noise caused by the electrical environment of the qubit [3,7–12]. Charge noise can be represented by voltage noise in the detuning of the qubit [11], which results in fluctuations in the exchange splitting J that affect the frequency of the exchange rotations and cause decoherence. The charge-based decoherence is a severe factor that limits the performance of the singlet-triplet qubits. Thus, there have been several proposals for mitigating its effects, including multielectron singlet-triplet qubits [13,14] and optimized gate sequences [15,16].

Another widely investigated possibility is to exploit the so-called sweet spot regions where the exchange splitting is insensitive to charge noise in the gate operations [9,11,14,17]. For example, in the far detuned region, where both the singlet and the triplet are in the doubly occupied charge states, the qubit is much less susceptible to charge noise as both of the qubit states have similar charge densities [11]. Utilizing this insensitive region for gate operations requires rapid switching between the sweet spot and the singly occupied configuration with one electron in each dot. To prevent excitation into higher orbital states during this transfer of one electron from one dot to another, the corresponding change in detuning needs to be adiabatic with respect to the tunnel coupling [18]. On the other hand, the phase accumulated in the doubly occupied configuration should be as small as possible (of order π) in order to minimize dephasing. Thus, the switching time should be on the order of $1/J$. Together with the adiabaticity requirement, this condition implies that the tunnel coupling must be larger than the exchange splitting. Furthermore, the limited speed of control electronics favors switching times not much faster than 1 ns so that exchange splittings exceeding a few μeV are practically cumbersome. On the other hand, singlet-triplet qubits typically employ a

Pauli blockade for readout via a spin to charge conversion, which requires an exchange splitting larger than the tunnel coupling to maintain good charge contrast. Hence, one faces two conflicting requirements: small J for high fidelity gates, but large J for the readout.

In this paper, we propose an asymmetric double quantum dot (ADQD) system, consisting of two quantum dots with different sizes, that allows exchange-gate operations with high tolerance to charge noise in the doubly occupied region of one dot while double occupation of the other dot is used for the readout (see Fig. 1). Using out of plane magnetic fields, the exchange splitting can be set to a small nonzero value for the exchange gate in the doubly occupied region of the larger dot. Due to the size difference, the exchange stays large in the smaller dot, which can be used in the projective readout of the system. Thus, the conflicting requirements outlined above can be met simultaneously. Note that asymmetric double quantum dots have been proposed previously in the context of the so-called inverted singlet-triplet qubits [19].

II. METHODS

The DQD two-electron system (confined to the xy plane) is described with the continuum Hamiltonian

$$\hat{H} = \sum_{j=1}^{2} \left[\frac{[\hat{\mathbf{p}}_j + e\mathbf{A}(\mathbf{r}_j)]^2}{2m^*} + V(\mathbf{r}_j) \right] + \frac{e^2}{4\pi\epsilon r_{12}}. \quad (1)$$

Here, $\mathbf{A}(\mathbf{r}_j) = \frac{1}{2} B_z(-y_j, x_j, 0)$ is the magnetic vector potential corresponding to a homogeneous external magnetic field B_z and V the electric potential. $m^* \approx 0.067 m_e$ and $\epsilon \approx 12.7\epsilon_0$ are the effective electron mass and permittivity in GaAs, respectively.

The electric potential $V(\mathbf{r}) = V(x,y) = V_c(x,y) + V_d(x,y)$ consists of the QD confinement V_c and the detuning potential V_d. We model the DQD system as two parabolical wells located at the x axis at $\mathbf{R}_1 = (-\frac{a}{2}, 0)$ and $\mathbf{R}_2 = (\frac{a}{2}, 0)$, where a is the distance of the QD minima. The detuning $V_d(x,y)$ is modeled as a step function that assumes the value $-\frac{\epsilon}{2}$ in the left dot (the one at the negative x axis) and the value $\frac{\epsilon}{2}$ in the right one, with
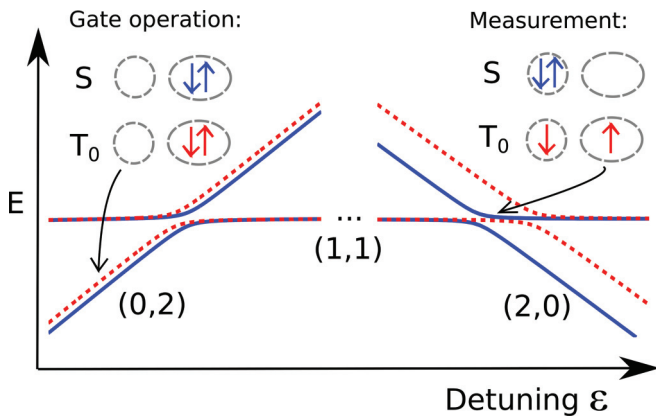
FIG. 1. (Color online) The ADQD scheme. The energies of the singlet (blue lines) and triplet (dashed red lines) are shown in the two dots [(0,2) and (2,0) configurations] as functions of the detuning of the dots ϵ. The exchange-gate operations are done in the larger right dot so that both the singlet and triplet are in the (0,2) configuration. The projective measurement is conducted using the smaller left dot, with the singlet in (2,0) and the triplet in (1,1).

$\epsilon = V(\mathbf{R}_2) - V(\mathbf{R}_1)$ being the energy difference between the dots.

The electric potential of the ADQD system is illustrated in Fig. 2. The potentials V_c, V_d, and $V = V_c + V_d$ are shown in the x axis. The minima of the dots are $a = 130$ nm apart, located on the x axis, at ± 65 nm. The confinement is piecewise parabolical, meaning that the confinement strength in the x direction has different values in different regions. The (singlet) intradot tunneling has the values 55 and 38 μeV at $B_z = 0$ and 0.87 T magnetic fields, respectively. The actual form of the dots (e.g., whether they are elliptical or circular) was not

found to have significant effects on the physics of the system. The piecewise quadratic form was chosen because it allows the control of the tunneling and the J splitting independently.

The Hamiltonian (1) is diagonalized using the exact diagonalization (ED) method and the Lanczos algorithm. In the Lanczos method, only the ground state and its energy are obtained accurately. The higher lying eigenstates can be obtained using a "ladder operation." The kth state $|\psi_k\rangle$ is obtained as the ground state of the Hamiltonian

$$H_k = H + \delta \sum_{s=1}^{k-1} |\psi_s\rangle\langle\psi_s|, \qquad (2)$$

where H is the original Hamiltonian of the system and $\delta > 0$ is a penalizing constant that moves the lower eigenstates $\{|\psi\rangle_s\}_{s=1}^{k-1}$ above the desired kth state.

In the ED many-body calculations, the one-particle basis consists of the eigenstates corresponding to the confinement potential V. The multiparticle basis is constructed from the single-particle basis as the antisymmetrized Fock states. The one-particle eigenstates $\{|\psi_p\rangle\}_{p=1}^{N_1}$ (the eigenbasis size being N_1) are computed using the multicenter Gaussian basis $\{|\phi_i\rangle\}_{i=1}^{N_g}$ (this method is described in detail by Nielsen *et al.* [17]). The electron-electron interaction matrix elements $V_{i,j,k,l} = \langle\phi_i|\langle\phi_j|\frac{1}{r_{12}}|\phi_l\rangle|\phi_k\rangle$ and the electric potential elements $V_{i,j} = \langle\phi_i|V_c(\mathbf{r})|\phi_j\rangle$ can be obtained analytically in this basis. The matrix elements $\tilde{V}_{p,q}$ and $\tilde{V}_{p,q,r,s}$ corresponding to the one-particle eigenstates are then computed from the Gaussian elements by basis changes.

In the computation of the one-particle eigenstates, $\{|\psi_p\rangle\}_{p=1}^{N_1}$, an evenly spaced grid of several hundred Gaussian functions (up to $N_g = 500$) is used. The grid dimensions and the Gaussian widths are optimized and the convergence of the states is verified by comparing the energies to ones obtained with a much larger grid. We perform the basis change corresponding to the elements $\tilde{V}_{p,q,r,s}$ with an Nvidia Tesla C2070 graphics processing unit, which was programed with CUDA, a parallel programming model for Nvidia GPUs. The many-body eigenstates are computed with ED using 50 first single-particle states ($N_1 = 50$). This basis size is found to be sufficient for the convergence of the results (the relative difference of the two-body singlet and triplet energies with 45 and 50 single-particle states is less than 0.1% up to very high detuning regions).

III. EXCHANGE GATES

A. Magnetic control of the exchange spiltting

In singlet-triplet qubits, the exchange interactions create an energy splitting $J = E_{T_0} - E_S$ between the singlet $|S\rangle$ and $S_z = 0$ triplet $|T_0\rangle$. When the qubit is in the (1,1)-charge configuration (i.e., one electron in each dot), the exchange is typically very close to zero, in the sub-μeV region. It can be turned on by detuning one of the dots of the DQD system to a lower potential. As the detuning is increased, it will eventually overcome the Coulomb repulsion and both electrons will localize to the dot with the lower potential. In the zero or low magnetic field, the $S = 0$ singlet is the ground state and the transition to the doubly occupied (2,0) and (0,2)
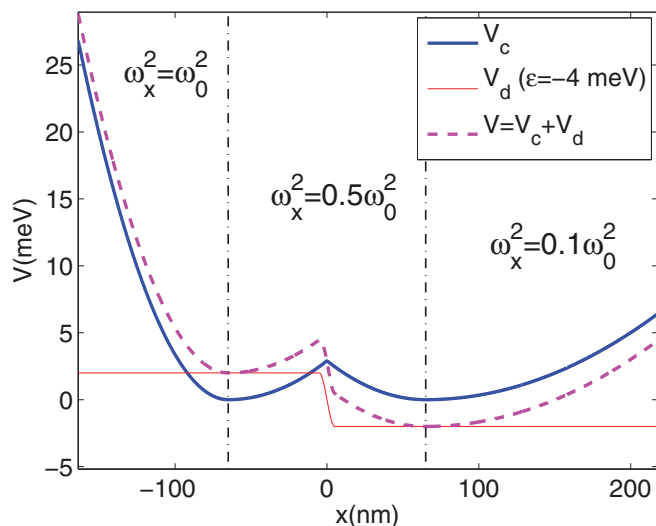

FIG. 2. (Color online) The electric potential in the x axis of the DQD system. The piecewise parabolic confinement V_c is shown as the blue line. The minima of the dots are at $x = \pm 65$ nm on the x axis and the confinement strength in the y direction is $\hbar\omega_0 = 2.5$ meV. The regions of different x confinements ω_x are shown with the dashed vertical lines. The detuning potential V_d, with $\epsilon = -4$ meV, is shown in red, and the combined electric potential $V = V_c + V_d$ as the dashed purple line.
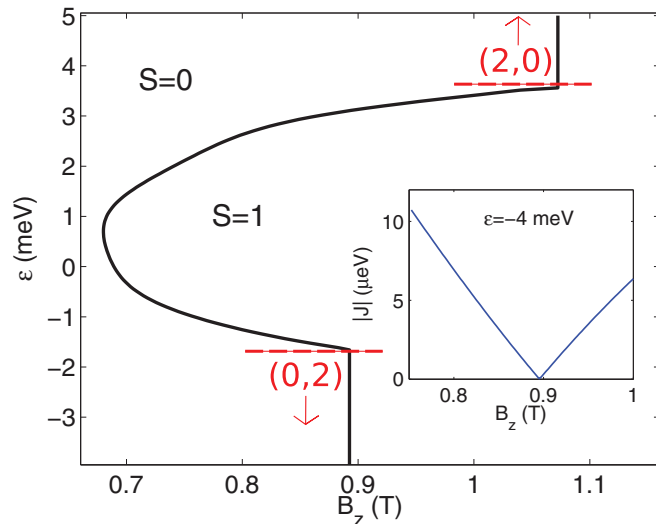
FIG. 3. (Color online) The ground state spin as a function of the magnetic field B_z and the detuning ϵ (negative values of ϵ correspond to the right dot in low potential and positive to the left dot) in the ADQD system of Fig. 2. The boundary curve between the $S = 0$ and $S = 1$ ground states is shown with the black line. The dashed red lines denote the boundaries of the regions where both the singlet and the triplet are in the doubly occupied charge states. Inset: The magnetic field dependence of the absolute value of the exchange energy J in the larger dot. Here, the detuning is $\epsilon = -4$ meV, corresponding to the region where both $|S\rangle$ and $|T_0\rangle$ are in the (2,0)-charge configuration.

states happens at lower detuning values in the $|S\rangle$ state than in the $|T_0\rangle$ state. However, increasing the B_z magnetic field will eventually shift the triplet as the ground state [20]. The ground state spin in the DQD system of Fig. 2 is plotted in Fig. 3 as a function of the magnetic field B_z and the detuning ϵ.

As seen in the figure, the spin phase boundary becomes a straight line at high detuning ($\epsilon < -2$ meV or $\epsilon > 4$ meV), i.e.,

the transition to the $S = 1$ ground state happens at a fixed value of B_z regardless of the detuning. This is due to the transition to the doubly occupied (2,0) and (0,2) states. When both the singlet and the triplet have undergone the transition, the system behaves as a doubly occupied single dot, and the detuning just lowers the energies E_S and E_{T_0} but keeps J (approximately) constant. In the figure, the transition value is $B_z = 0.893$ T in the right dot and $B_z = 1.07$ T in the smaller left dot. The transition values of B_z depend on the confinement strengths of the dots. The larger the dot, the lower is the transition value. Along the transition boundary, the $|S\rangle$ and $|T_0\rangle$ states are degenerate.

The ADQD system allows the implementation of single-qubit exchange gates that are operated in the doubly occupied region with a magnetically controllable value of J. The perpendicular magnetic field is set to a value that is close to the $S = 1$ transition in the larger dot to obtain a J splitting of a few μeVs (smaller than the intradot tunneling) in the doubly occupied (0,2) region of the larger right dot. We found that in the zero magnetic field, one would need to have very large dots with wave function diameters close to 1 μm to quench J this small in the doubly occupied region.

The inset in Fig. 3 shows the absolute value of the exchange energy in the doubly occupied region of the larger right dot as a function of the magnetic field B_z. Here, the detuning is $\epsilon = -4$ meV, corresponding to the region where both the singlet and the triplet are in the (0,2)-charge configuration. As seen in the figure, J is approximately linear in B_z close to the $S = 1$ transition values. At the spin phase boundary (at $B_z = 0.893$ T), J changes sign, i.e., the triplet becomes the ground state, as seen in the kink at the $|J|$ curve of the inset.

B. Protection against charge noise

The $|S(0,2)\rangle$ and $|T_0(0,2)\rangle$ states have close to identical charge densities, as shown in the the left panels of Fig. 4, allowing protection against electrical noise. The charge
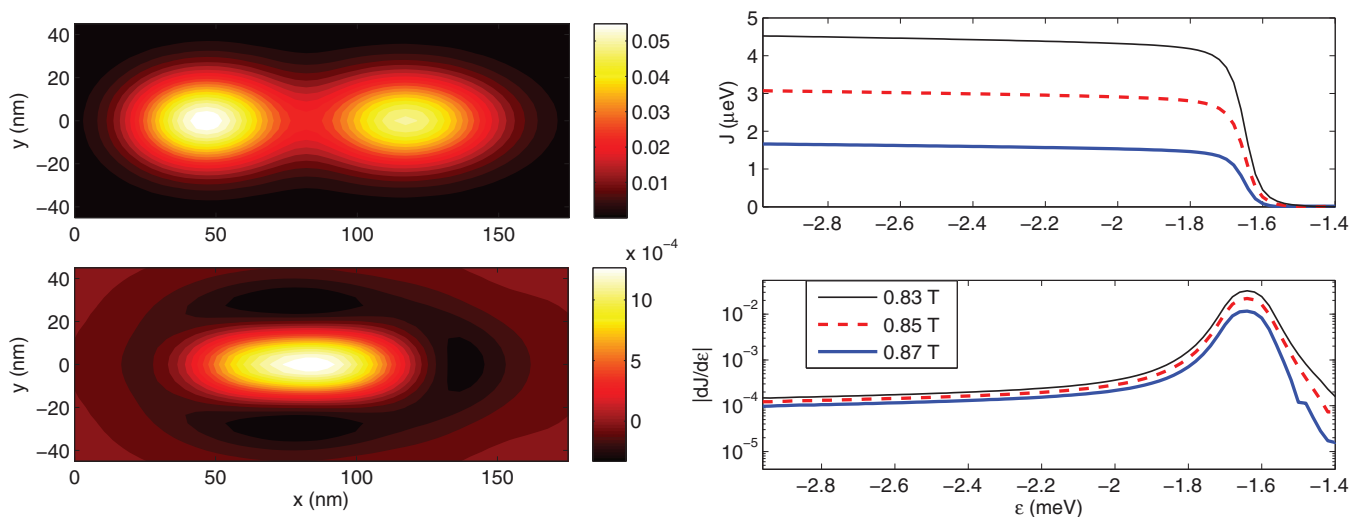

FIG. 4. (Color online) Left: The charge density of the singlet ρ_S (the upper plot) and the difference of the singlet and the triplet $\rho_S - \rho_{T_0}$ (the lower plot) in the (0,2) configuration with the magnetic field strength $B_z = 0.87$ T (the states are localized in the right dot, so the left dot is omitted in the pictures). The ADQD-system parameters are as in Fig. 2. The detuning is $\epsilon = -4$ meV, corresponding to an exchange energy of $J = 1.7$ μeV. Here, the unit of the densities is e/nm^2. Right: The exchange energy J (upper plot) and its derivative $dJ/d\epsilon$ (lower plot) as functions of the detuning ϵ. The results are shown with several values of B_z taken near the spin phase transition at $B_z = 0.893$.

difference between the singlet and the triplet in the left dot is $\Delta q^{\text{right}} = q_S^{\text{right}} - q_{T_0}^{\text{right}} = 4.7 \times 10^{-5}e$ (obtained by integrating the difference of the lower plot). This is in stark contrast to the traditional exchange-gate implementation, where the gate is operated near the singlet (0,2) transition while the triplet stays fully in (1,1). In this case, the charge difference (corresponding to the same J value as in the doubly occupied case above) is $\Delta q^{\text{right}} = q_S^{\text{right}} - q_{T_0}^{\text{right}} = 2.7 \times 10^{-2}e$, more than three orders of magnitude larger. In the (0,2) configuration, the qubit states are also protected from the hyperfine induced decoherence, as both electrons are localized in the same dot and the hyperfine effects are suppressed under exchange [3]. In the (1,1) configuration, the qubit is still susceptible to hyperfine decoherence completely similarly to the regular S-T_0 qubits. The asymmetry of the dots should not cause effects in this regard.

Decoherence by charge noise in S-T_0 qubits has been measured to behave as ϵ noise [11], meaning that charge noise manifests itself as effective fluctuations in the qubit's detuning ϵ. The decoherence from charge noise is thus mainly governed by $|dJ/d\epsilon|$. The right panels of Fig. 4 show J and its derivative $|dJ/d\epsilon|$ as a function of the detuning ϵ. As seen in the figures, J stays approximately constant after the charge transitions ($\epsilon < -2$ meV). There is, however, a small, close to linear, ϵ dependence even in the (0,2) region. This is explained by the fact that the wave functions of the singlet and triplet have small finite values in the barrier between the dots. The residual dependence can be decreased by lowering the intradot tunneling, i.e., increasing the barrier between the dots (the tunneling value in the system of Fig. 2 is quite large; 55 and 38 μeV at $B_z = 0$ and 0.87 T magnetic fields, respectively). The actual form of the confinement may also have quantitative effects [21], but these are expected to be negligible as the amplitude of the wave function tail in the barrier, depending mainly on the barrier width and height, is very small in a typical singlet-triplet qubit operation.

In any case, the values of $|dJ/d\epsilon|$ in this proposed (0,2) operation stay much lower than in the corresponding traditional $S(0,2)$-$T_0(1,1)$ exchange gates. For example, in the $B_z = 0.850$ T curve that corresponds to $J = 3.07$ μeV, the derivative has the value $|dJ/d\epsilon| = 1.26 \times 10^{-4}$. If one were to create the same exchange splitting $J = 3.07$ μeV in the (1,1)-(0,2) transition region, the derivative would be several hundred times larger, $|dJ/d\epsilon| = 2.59 \times 10^{-2}$, corresponding to the case where the smaller dot in Fig. 2 is detuned to low energy in $B_z = 0$. In the bigger dot or nonzero fields, the derivative would be even larger, as the S-T_0 splitting stays smaller, and larger charge density differences are needed for the same exchange splitting.

The loss of coherence for a given pulse sequence, evolution time, and noise spectrum, which is the ultimate figure of merit for qubit operations, can be shown to be proportional to $(dJ/d\epsilon)^2$ [9,22]. Thus, we find that an improvement of two orders of magnitude is possible. When considering dephasing times, $dJ/d\epsilon$ enters linearly for T_2^* arising from quasistatic noise, and quadratically for T_2^* arising from white noise. In the former case, the coherence time can be computed as [11,23]

$$T_2^* = \frac{\sqrt{2}\hbar}{\frac{dJ}{d\epsilon}\epsilon_{\text{rms}}}, \qquad (3)$$

where ϵ_{rms} is the root-mean-squared fluctuation of the detuning. For example, in the paper by Dial *et al.* in Ref. [11], $\epsilon_{\text{rms}} = 1$ μeV, taking into account a lever arm of order 0.1 for converting gate voltages to detuning. Using this value and the derivative values corresponding to $J = 3.07$ μeV, $|dJ/d\epsilon| = 1.275 \times 10^{-4}$, and $|dJ/d\epsilon| = 2.594 \times 10^{-2}$, one obtains the coherence times $T_2^* = 30$ ns and $T_2^* = 6.2$ μs in the (1,1) and (0,2) operations, respectively. The fidelity of a π pulse around the z axis in the Bloch sphere is then given as [11]

$$f(T_\pi) = \exp\left[-\left(\frac{\hbar\pi}{JT_2^*}\right)^2\right], \qquad (4)$$

giving $1 - f(T_\pi) = 1.2 \times 10^{-8}$ in the (0,2) operation, while the (1,1) operation gives $1 - f(T_\pi) = 5.1 \times 10^{-4}$ ($f \equiv 1$ for ideal processes; noisy time evolutions lower f to magnitudes smaller than 1).

IV. PROJECTIVE READOUT

Next, we discuss the projective readout [3,9] of the ADQD system done in the smaller left dot. The singlet probability is measured by sweeping the detuning to a region where only the singlet is in the doubly occupied configuration. The difference in the values of B_z corresponding to the $S = 1$ transition in (2,0) and (0,2) allows the smaller dot to have large J values and charge density differences between the qubit states, while in the right dot the doubly occupied states are nearly degenerate. The anticrossing of the charge states in the left dot for the same system as in Figs. 3 and 4 is shown in Fig. 5. Between the singlet and triplet anticrossings (3.45 meV $< \epsilon <$ 3.70 meV),
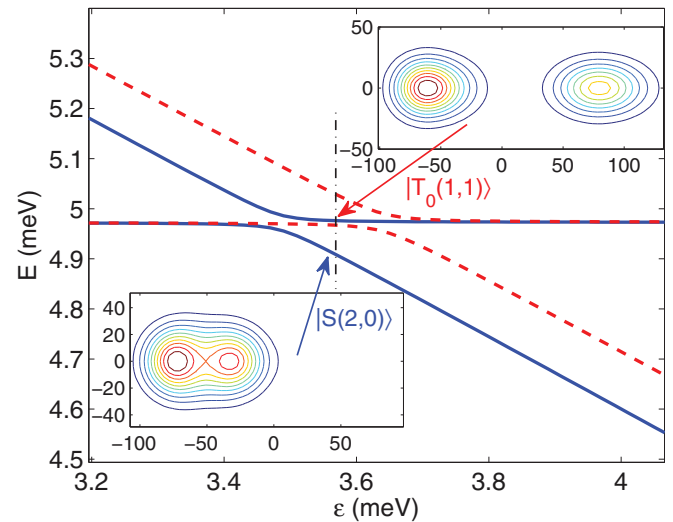

FIG. 5. (Color online) The energies of the lowest singlet and triplet states at their charge transition anticrossings in the smaller left dot of the ADQD system of Fig. 2. The magnetic field is $B_z = 0.87$ T, which corresponds to close to identical charge densities in the larger dot (see Fig. 4). The singlet states are shown with blue lines and the triplets with red dashed lines. The insets show the densities (the unit is e/nm^2) of the lowest $|S\rangle$ and $|T_0\rangle$ states taken at $\epsilon = 3.57$ meV (denoted by the arrows and the dashed-dotted vertical line in the figure).

there is a region where the singlet is fully in (2,0) while the triplet is in (1,1). The insets in the left panel show the singlet and triplet charge densities taken at $\epsilon = 3.57$ meV between the anticrossings. In the insets, the amount of charge in the right dot is $q_{T_0}^{\text{right}} = 0.900e$ in the triplet and $q_S^{\text{right}} = 0.0993e$ in the singlet.

We find from additional simulations that tighter confinement allows a better "performance" in terms of the measurement. In these smaller systems (e.g., a system with $a = 80$ nm and $\hbar\omega_0 = 4$ meV), the distance between the singlet and triplet (0,2) anticrossings is relatively larger. Thus there are regions between the anticrossings where S is fully in (2,0) (q_S^{right} is very close to zero) while $|T_0\rangle$ still has not started to undergo its transition ($q_{T_0}^{\text{right}}$ is very close to one). Also, quenching the tunneling will make the anticrossing area effectively larger. However, a too small tunneling can lead to leakage problems when sweeping the system from (2,0) to (0,2) [18].

V. QUBIT OPERATION

Finally, we will shortly discuss general gate operation in ADQD singlet-triplet qubits. The x rotations in the Bloch sphere are generated with magnetic field gradients as in the conventional S-T_0 qubits [5]. The magnetic field gradient between the two dots of the system can be simulated by adding a Zeemann term $V_Z(\mathbf{r}) = g^* \mu_B B_{\text{nuc}}(\mathbf{r})S_z$ to the Hamiltonian of Eq. (1). Here, the inhomogeneous magnetic field B_{nuc} is modeled as a step function that assumes constant values at each dot. As expected, these additional simulations show that the x rotations done in the (1,1)-charge configuration are found to work completely similarly to the conventional case. The two-qubit operations can also be implemented the same way as conventionally: capacitatively [using the smaller dot and the "typical" $S(0,2)$-$T_0(1,1)$ detuning regime] [2,6,24] or with exchange based methods [1,25]. The latter would benefit from the improved charge-noise resilience discussed here. There has also been a proposal for using the double occupation region in capacitive coupling [26], which could offer large enhancements to the coherence times in the two-qubit operation. This scheme could also benefit from the ADQD S-T_0 qubit implementation and the magnetic field control of J, as it would allow the quenching of J to the subtunneling scale.

The z rotations done in the deep (2,0) region require fairly large detuning pulses to move the system between the (2,0) and (0,2) regions. A too fast detuning pulse can lead to charge state leakage that can be mitigated by enhancing the tunneling. In the system studied, the tunneling is 38 μeV in the field $B_z = 0.87$ T. Assuming linear detuning pulses and Landau-Zener type transitions, we find that the leakage in the detuning sweep from $\epsilon = -3$ to 4 meV is negligible if the pulse duration is above 5 ns. In experiments, however, the pulses are not linear, instead they can be faster in the regions where J grows slowly [5], allowing shorter overall durations. As the magnetic field is found to quench the tunneling value between the dots, the ADQD scheme might require somewhat shorter dot distances than the conventional S-T_0 qubits operated in low magnetic fields to ensure large enough tunneling.

A potential difficulty when implementing the ADQD scheme discussed in this paper is that since J is independent of detuning, the rotation angle of a gate cannot be controlled by the pulse amplitude. Instead, the pulse duration must be used, which is less flexibly controllable on current pulse generators. Furthermore, larger voltage pulses spanning all the way from (0,2) to (2,0) are required for readout.

VI. SUMMARY

We have simulated a singlet-triplet qubit based on an asymmetric double quantum dot system. The size difference of the dots allows the larger one to be used in exchange-gate operations with a moderate and controllable J splitting done in the far detuned (0,2) regime, while when detuning the smaller dot to low potential, the splitting stays large enough for the projective readout of the qubit. In the far (0,2) regime, the S and T_0 states have similar charge densities which results in weaker coupling between the qubit and its charge environment. The detuning dependence of J was found to be very small in the (0,2) region, resulting in high resistance to ϵ noise, which is the dominant form of charge noise. The ADQD scheme allows for a noise resistant implementation of exchange gates in singlet-triplet qubits, alleviating the crucial problem of decoherence in this quantum computing architecture.

[1] J. Levy, Universal quantum computation with spin-1/2 pairs and heisenberg exchange, Phys. Rev. Lett. **89**, 147902 (2002).

[2] J. M. Taylor, H. A. Engel, W. Dür, A. Yacoby, C. M. Marcus, P. Zoller, and M. D. Lukin, Fault-tolerant architecture for quantum computation using electrically controlled semiconductor spins, Nat. Phys. **1**, 177 (2005).

[3] J. R. Petta, A. C. Johnson, J. M. Taylor, E. A. Laird, A. Yacoby, M. D. Lukin, C. M. Marcus, M. P. Hanson, and A. C. Gossard, Coherent manipulation of coupled electron spins in semiconductor quantum dots, Science **309**, 2180 (2005).

[4] R. Hanson and G. Burkard, Universal set of quantum gates for double-dot spin qubits with fixed interdot coupling, Phys. Rev. Lett. **98**, 050502 (2007).

[5] S. Foletti, H. Bluhm, D. Mahalu, V. Umansky, and A. Yacoby, Universal quantum control of two-electron spin quantum bits using dynamic nuclear polarization, Nat. Phys. **5**, 903 (2009).

[6] M. D. Shulman, O. E. Dial, S. P. Harvey, H. Bluhm, V. Umansky, and A. Yacoby, Demonstration of entanglement of electrostatically coupled singlet-triplet qubits, Science **336**, 202 (2012).

[7] X. Hu and S. Das Sarma, Charge-fluctuation-induced dephasing of exchange-coupled spin qubits, Phys. Rev. Lett. **96**, 100501 (2006).

[8] I. van Weperen, B. D. Armstrong, E. A. Laird, J. Medford, C. M. Marcus, M. P. Hanson, and A. C. Gossard, Charge-state conditional operation of a spin qubit, Phys. Rev. Lett. **107**, 030506 (2011).

[9] J. M. Taylor, J. R. Petta, A. C. Johnson, A. Yacoby, C. M. Marcus, and M. D. Lukin, Relaxation, dephasing, and quantum control of electron spins in double quantum dots, Phys. Rev. B **76**, 035315 (2007).

[10] B. M. Maune, M. G. Borselli, B. Huang, T. D. Ladd, P. W. Deelman, K. S. Holabird, A. A. Kiselev, I. Alvarado-Rodriguez, R. S. Ross, A. E. Schmitz *et al.*, Coherent singlet-triplet oscillations in a silicon-based double quantum dot, Nature (London) **481**, 344 (2012).

[11] O. E. Dial, M. D. Shulman, S. P. Harvey, H. Bluhm, V. Umansky, and A. Yacoby, Charge noise spectroscopy using coherent exchange oscillations in a singlet-triplet qubit, Phys. Rev. Lett. **110**, 146804 (2013).

[12] G. Ramon and X. Hu, Decoherence of spin qubits due to a nearby charge fluctuator in gate-defined double dots, Phys. Rev. B **81**, 045304 (2010).

[13] E. Barnes, J. P. Kestner, N. T. T. Nguyen, and S. Das Sarma, Screening of charged impurities with multielectron singlet-triplet spin qubits in quantum dots, Phys. Rev. B **84**, 235309 (2011).

[14] S. Mehl and D. P. DiVincenzo, Noise-protected gate for six-electron double-dot qubit, Phys. Rev. B **88**, 161408 (2013).

[15] J. P. Kestner, X. Wang, L. S. Bishop, E. Barnes, and S. Das Sarma, Noise-resistant control for a spin qubit array, Phys. Rev. Lett. **110**, 140502 (2013).

[16] P. Cerfontaine, T. Botzem, D. P. DiVincenzo, and H. Bluhm, High-fidelity single-qubit gates for two-electron spin qubits in gaas, Phys. Rev. Lett. **113**, 150501 (2014).

[17] E. Nielsen, R. W. Young, R. P. Muller, and M. S. Carroll, Implications of simultaneous requirements for low-noise exchange gates in double quantum dots, Phys. Rev. B **82**, 075319 (2010).

[18] T. Hiltunen, J. Ritala, T. Siro, and A. Harju, Non-adiabatic charge state transitions in singlettriplet qubits, New J. Phys. **15**, 103015 (2013).

[19] S. Mehl and D. P. DiVincenzo, Inverted singlet-triplet qubit coded on a two-electron double quantum dot, Phys. Rev. B **90**, 195424 (2014).

[20] A. Harju, S. Siljamäki, and R. M. Nieminen, Two-electron quantum dot molecule: Composite particles and the spin phase diagram, Phys. Rev. Lett. **88**, 226804 (2002).

[21] Q. Li, Ł. Cywiński, D. Culcer, X. Hu, and S. Das Sarma, Exchange coupling in silicon quantum dots: Theoretical considerations for quantum computation, Phys. Rev. B **81**, 085313 (2010).

[22] G. Ithier, E. Collin, P. Joyez, P. J. Meeson, D. Vion, D. Esteve, F. Chiarello, A. Shnirman, Y. Makhlin, J. Schriefl, and G. Schön, Decoherence in a superconducting quantum bit circuit, Phys. Rev. B **72**, 134519 (2005).

[23] H. Ribeiro, G. Burkard, J. R. Petta, H. Lu, and A. C. Gossard, Coherent adiabatic spin control in the presence of charge noise using tailored pulses, Phys. Rev. Lett. **110**, 086804 (2013).

[24] D. Stepanenko and G. Burkard, Quantum gates between capacitively coupled double quantum dot two-spin qubits, Phys. Rev. B **75**, 085324 (2007).

[25] R. Li, X. Hu, and J. Q. You, Controllable exchange coupling between two singlet-triplet qubits, Phys. Rev. B **86**, 205306 (2012).

[26] E. Nielsen, R. P. Muller, and M. S. Carroll, Configuration interaction calculations of the controlled phase gate in double quantum dot qubits, Phys. Rev. B **85**, 035319 (2012).